Published in final edited form as:
Matrix Biol. 2012 May ; 31(4): 253–260. doi:10.1016/j.matbio.2012.02.001.

Sulfatases are determinants of alveolar formation

Emilio Arteaga-Solis[1,2], **Carmine Settembre**[1,3], **Andrea Ballabio**[3,4], and **Gerard Karsenty**[1,5]

[1]Department of Genetics and Development, Columbia University, New York, New York 10032, USA

[2]Division of Pediatric Pulmonary College of Physicians and Surgeons, Columbia University, New York, New York 10032, USA

[3]Telethon Institute of Genetics and Medicine (TIGEM), Naples 80131, Italy

[4]Medical Genetics, Department of Pediatrics, Federico II University, Naples 80131, Italy

Abstract

Alveolar formation or alveolarization is orchestrated by a finely regulated and complex interaction between growth factors and extracellular matrix proteins. The lung parenchyma contains various extracellular matrix proteins including proteoglycans, which are composed of glycosaminoglycans (GAGs) linked to a protein core. Although GAGs are known to regulate growth factor distribution and activity according to their degree of sulfation the role of sulfated GAG in the respiratory system is not well understood. The degree of sulfation of GAGs is regulated in part, by sulfatases that remove sulfate groups. In vertebrates, the enzyme Sulfatase-Modifying Factor 1 (Sumf1) activates all sulfatases. Here we utilized mice lacking *Sumf1*$^{-/-}$ to study the importance of proteoglycan desulfation in lung development. The *Sumf1*$^{-/-}$ mice have normal lungs up until the onset of alveolarization at post-natal day 5 (P5). We detected increased deposition of sulfated GAG throughout the lung parenchyma and a decrease in alveolar septa formation. Moreover, stereological analysis showed that the alveolar volume is 20% larger in *Sumf1*$^{-/-}$ as compared to wild type (WT) mice at P10 and P30. Additionally, pulmonary function test were consistent with increased alveolar volume. Genetic experiments demonstrate that in *Sumf1*$^{-/-}$ mice arrest of alveolarization is independent of fibroblast growth factor signaling. In turn, the *Sumf1*$^{-/-}$ mice have increased transforming growth factor β (TGFβ) signaling and *in vivo* injection of TGFβ neutralizing antibody leads to normalization of alveolarization. Thus, absence of sulfatase activity increases sulfated GAG deposition in the lungs causing deregulation of TGFβ signaling and arrest of alveolarization.

Keywords

Alveolarization; Sumf1; Glycosaminoglycans; Sulfatases; TGFβ

1. Introduction

Alveolarization is driven by a complex interplay between extracellular matrix proteins (ECM) and secreted growth factors (Roth-Kleiner and Post, 2005). The alveolar ECM is

[5]Corresponding Author: Gerard Karsenty, MD, PhD, Gk2172@columbia.edu, Phone: 12-305-6398, Fax: 212-923-2090.

composed of type IV collagen, laminin, entactin/nidogen, tenascin, integrins, elastin, fibrillins and proteoglycans (Galambos and Demello, 2008). Proteoglycans (PG) are composed of a protein core to which one or more highly sulfated polysaccharide chains, known as glycosaminoglycans (GAG), bind. The PGs help stabilize the three-dimensional fibrillar matrix providing resistance to tissue compression and interstitial fluid expansion. In addition, the GAGs moieties of proteoglycans are known to regulate a myriad of functions in organ growth, and cell differentiation and proliferation. Those functions are mediated through their ability to bind a diverse repertoire of signaling molecules (Esko and Lindahl, 2001). This essential aspect of GAGs is dependent on their degree of sulfation that is determined by sulfotransferases that incorporate the sulfated groups, and the sulfatases that remove them (Bulow and Hobert, 2006; Diez-Roux and Ballabio, 2005).

Vertebrates have at least 17 different sulfatases, whose functions are determined by their subcellular localization and substrate specificity (Diez-Roux and Ballabio, 2005). Activation of all sulfatases requires a posttranslational formylglycination catalyzed by the enzyme Sulfatase-Modifying Factor 1 (Sumf1) (Cosma et al., 2003). Hence, Sumf1 is viewed as the master regulator of proteoglycan desulfation (Diez-Roux and Ballabio, 2005). In humans, mutations in various sulfatases or in *Sumf1* are known to cause a broad spectrum of diseases that include the mucopolysaccharidoses where lack of lysosomal sulfatases leads to intra-lysosomal accumulation of GAG due to blockage of GAG degradation (Diez-Roux and Ballabio, 2005). Sumf1 deficiency, in humans, causes multiple sulfatase deficiency, which is a rare disease that encompasses all the phenotypic findings in the diseases caused by individual sulfatases (Cosma et al., 2003). Although, patients with multisulfatase deficiency develop among other symptoms poorly characterized breathing abnormalities the role of sulfatases during lung development is not well characterized.

To define the importance of proteoglycan desulfation during lung development we studied mice lacking *Sumf1*$^{-/-}$ (Settembre et al., 2007). We show here that in the absence of *Sumf1,* resulting in increase proteoglycan sulfation in the lungs, there is a developmental arrest in alveolar formation that alters lung function. Further evidence shows that *Sumf1* regulation of alveolarization occurs by the deregulation of TGFβ and not FGF signaling.

2. Results

2.1. Proteoglycan desulfation affects alveolar formation

To characterize the importance of desulfation in lung development we embarked in a systematic histomorphometrical analysis of the *Sumf1*$^{-/-}$ lungs from embryonic day 12.5 to adulthood. Analysis at various embryonic stages, at birth and at P5 failed to demonstrate any difference in bronchial patterning or lobe formation (data not shown and Figure 1a). At P10 however, we observed an increase in distal airspace caliber in *Sumf1*$^{-/-}$ compared to WT mice (Figure 1a) consistent with a disruption in alveolar septation. The *Sumf1*$^{-/-}$ mice had rare secondary alveolar septa (Fig 1a insert), but their proximal airway caliber and vasculature appeared grossly normal. This increase in distal airway caliber persisted at P30, after the conclusion of normal alveolar septation in mice (Figure 1a). To quantify alveolar size and number of alveolar septa we used stereological techniques on methylmethacrylate embedded lungs as this is known to provide a more accurate representation of the three-dimensional alveolar volume compared to the more commonly used mean linear intercept (Ochs, 2006). Calculation of alveolar volume and surface area at P5, P10, P30 showed progressive distal airspace enlargement in the mutant mice. This is evident from a 20% increase in alveolar volume and a 40% decrease in alveolar surface area in the *Sumf1*$^{-/-}$ compared to WT mice at P10 and P30 (Figure 1b). In addition, at P10 there was a 75% reduction in the number of alveolar septa per given area in the *Sumf1*$^{-/-}$ compared to WT mice (Figure 1b). The ratio of lung volume, determined by volume displacement, to body

weight argued against overt lung hypoplasia as there was an increase in lung volume/body weight (30% at P10 and 35% at P30) (Figure 1c). Verhoeff elastic stain demonstrated normal elastic staining in the alveolar wall and secondary alveolar septa in the *Sumf1*$^{-/-}$ compared to WT mice (Figure 1d). Furthermore, there was no overt inflammation observed as there was no increase in neutrophil, monocyte or macrophage infiltration based on morphological analyses (data not shown). Thus, the lung phenotype associated with deficiency in Sumf1 is most consistent with a developmental perturbation of distal alveolar septation rather than a destructive process.

2.2. Sumf1$^{-/-}$ mice have altered lung function consistent with increased alveolar size

To investigate the physiological consequence of decreased alveolar septation in *Sumf1*$^{-/-}$ mice we utilized the forced oscillation technique (FlexiVent). We first used a sinusoidal forced oscillation waveform (SnapShot-150) to obtain total respiratory system dynamic resistance to airflow (R), elastance or elastic rigidity (E) and compliance (C). In the SnapShot perturbation, the lung is seen as a single compartment; hence, the R, E, and C represent the lung and the chest wall. As it is seen in an emphysematous lung, *Sumf1*$^{-/-}$ mice demonstrated a 27% decrease in R ($p<0.0001$), 30% decrease in E ($p<0.001$), and a 42% increase in C ($p<0.001$) (Figure 2a). These results were further confirmed by a constant-phase model or primewave-8 perturbation. In the primewave-8 perturbation, the lung is seen as a multiple compartment allowing the exclusion of the chest wall and the measurement of airway resistance (Raw), lung tissue damping (G) and lung tissue elastance (H). Again, consistent with alveolar enlargement there was a 14% decrease in Raw ($p<0.01$), a 30% decrease in G, and a 27% decrease in H (Figure 2b). These results indicate that the *Sumf1*$^{-/-}$ mouse lung has similar physiological properties as a lung with emphysema (Vanoirbeek et al., 2010); however, the “emphysema like” phenotype in the *Sumf1*$^{-/-}$ mice is the result of a developmental arrest.

2.3. Increased deposition of sulfated GAG and fibroblast growth factor (FGF)-independent arrest in alveolarization in the Sumf1$^{-/-}$ lung

The sulfated state of glycosaminoglycans is known to mediate its regulatory role in growth factor signaling (Lin, 2004). As expected, in the *Sumf1*$^{-/-}$ there is increased accumulation of sulfated glycosaminoglycans detected by acidic alcian blue staining that specifically stains hyper-sulfated glycosaminoglycans in the intra- or extra-cellular space (Figure 3a). In addition, biochemical analysis revealed a 67% increase in the levels of sulfated glycosaminoglycans in the lungs of *Sumf1*$^{-/-}$ compared to WT (Figure 3b). Since we have demonstrated that in the *Sumf1*$^{-/-}$ growth plate FGF18 signaling is increased (Settembre et al., 2008) and FGF signaling is a regulator of alveolar formation we asked whether FGF signaling was implicated in the development of the lung phenotype in *Sumf1*$^{-/-}$.

We first used a genetic approach to determine if FGF signaling was involved in mediating the phenotype observed in *Sumf1*$^{-/-}$ mice. We reasoned that an increase in FGF signaling in the lung may have a similar phenotype as no FGF signaling such as in the double FGF receptor 3 and FGF receptor 4 (*FGFR3*$^{-/-}$;*FGFR4*$^{-/-}$) homozygous or *FGF18*$^{-/-}$ mice where there is alveolarization arrest (Usui et al., 2004; Weinstein et al., 1998). In an attempt to decrease FGF signaling in *Sumf1*$^{-/-}$ mice we generated *Sumf1*$^{-/-}$ mice lacking one allele of the FGF18 (*Sumf1*$^{-/-}$;*FGF18*$^{+/-}$)or FGFR3 (*Sumf1*$^{-/-}$;*FGFR3*$^{+/-}$). Histologically, there was no difference between *Sumf1*$^{-/-}$ and *Sumf1*$^{-/-}$;*FGF18*$^{+/-}$ lungs (Fig 3c). Furthermore, stereological analysis of the lung failed to detect a difference in alveolar volume or surface area between *Sumf1*$^{-/-}$ and *Sumf1*$^{-/-}$;*FGF18*$^{+/-}$ mice (Fig 3d,e). Similarly, no differences were observed between *Sumf1*$^{-/-}$ and *Sumf1*$^{-/-}$;*FGFR3*$^{+/-}$ mice (data not shown). Taken together these experiments suggested that the mechanism by which the degree of sulfation affects lung formation is FGF18 and FGFR3-independent.

2.4. TGFβ signaling is affected in the Sumf1$^{-/-}$ mice

To further investigate the pathophysiology of the lung phenotype in *Sumf1*$^{-/-}$ mice we next looked at TGFβ signaling, a physiologic inhibitor of alveolar septation, which is up-regulated in various models of alveolar formation arrest (Dasgupta et al., 2009; Nakanishi et al., 2007; Neptune et al., 2003). We first detected increased Smad2 staining in *Sumf1*$^{-/-}$ compared to WT lungs at P5 (Fig 4a). Western blot analysis demonstrated that p-Smad2 levels were normal at P0 but significantly increased in *Sumf1*$^{-/-}$ compared to WT lungs at P5 (2 fold) and P10 (3 fold) suggesting that TGFβ signaling was increased in *Sumf1*$^{-/-}$ mice (Fig 4b,c). To test whether decreasing the levels of TGFβ *in vivo* would correct the lung phenotype seen in *Sumf1*$^{-/-}$ mice, pregnant *Sumf1*$^{+/-}$ mice were injected with TGFβ neutralizing antibodies prenatally. These antibodies neutralize the activity of TGFβ 1 and 2 both *in vivo* and *in vitro,* and *in utero* administration was demonstrated to rescue alveolarization post-natally (Tomita et al., 1998; Yamamoto et al., 1999; Neptune et al., 2003). Histologically, TGFβ neutralization led to an improvement of alveolar septation at P7 and P10 in *Sumf1*$^{-/-}$ mice (Fig 5a). There was no statistically significant difference in alveolar volume and surface area in *Sumf1*$^{-/-}$ compared to WT mice treated with TGFβ neutralizing antibodies (Fig 5b). As a negative control we injected mice with rabbit IgG and saw no such effect (Fig 5b). Consistent with prior observation, we detected a statistically significance difference in alveolar volume and surface area in WT mice treated with TGFβ neutralizing antibodies compared to rabbit IgG treated mice at P7; however, we failed to detect a significant difference at P10 (Fig 5a & b). Western analysis demonstrated normal levels of pSmad in *Sumf1*$^{-/-}$ lungs treated with TGFβ neutralizing antibodies compared to WT controls at P5 and P7 (Fig 5c & d). Finally, *Sumf1*$^{-/-}$ mice treated with TBFβ neutralizing antibodies had normal lung function at P20. In summary, these results demonstrate that in the absence of Sumf1 the increased levels of sulfated GAG in the lungs lead to an increase in TGFβ signaling.

3. Discussion

Absence of sulfatase activity leading to accumulation of sulfated GAG in the lung causes a disruption of alveolarization in a mouse model of multiple sulfatase deficiency, the *Sumf1*$^{-/-}$ mice. These mutant mice have increased distal airspace enlargement after the onset of alveolarization with no overt inflammation or tissue damage consistent with a developmental failure of alveolar septation. Consistent with the enlarged alveoli the lungs of *Sumf1*$^{-/-}$ mice have similar functional features as lungs with emphysema.

Alveolar septation, which is the last stage of lung development and in mice begins postnatally at P5, is regulated by various growth factors including members of the fibroblast growth factor (FGF) and transforming growth factor-β (TGFβ) family. Sulfated GAGs regulate the activity of the FGF and TGF-β family members (Kovensky, 2009; Schultz and Wysocki, 2009). FGFs are low molecular weight polypeptides whose signaling is mediated by FGF tyrosine kinase receptors (FGFR). During postnatal life, FRFR-3 and FGFR-4 play an essential role in regulating alveolarization (Weinstein et al., 1998). Indeed *FGFR-3*$^{-/-}$*;FGFR-4*$^{-/-}$ mice lack secondary septae formation and alveolarization resulting in enlarged airways (Weinstein et al., 1998). FGF18 have been implicated in postnatal lung development as it has high affinity for FGFR-3 and FGFR-4, is highly expressed during alveolarization and stimulates myofibroblast proliferation and differentiation (Chailley-Heu et al., 2005; Faham et al., 1996). Furthermore, FGF18 deletion in mice was reported to affect alveolarization (Usui et al., 2004); however, this analysis was conducted up to embryonic stage 18.5, prior to the onset of alveolar formation. GAGs are known to promote FGF signaling in particularly via the tri-sulfated disaccharide units of heparan sulfate chains (Frese et al., 2009; Kovensky, 2009; Lamanna et al., 2008). In fact, our prior study demonstrated that in *Sumf1*$^{-/-}$ mice FGF signaling was increased in chondrocyte and

removal of one FGF18 allele (*Sumf1*$^{-/-}$;*FGF18*$^{+/-}$ mice) was sufficient to rescue the skeletal phenotype (Settembre et al., 2008). Thus, we hypothesized that up regulation of FGF signaling in the lung may be causing the lung phenotype of the *Sumf1*$^{-/-}$ mice. However, genetic experiments demonstrated that the arrest in alveolar formation in the *Sumf1*$^{-/-}$ mice is FGF-independent.

TGFβ modulates multiple cellular processes including alveolar formation (Massague et al., 2000; Sporn and Roberts, 1992). TGFβ over expression in neonatal rats inhibits alveolar septation resulting in a bronchopulmonary dysplastic-like lung (Grande, 1997). Similar results were obtained in transgenic mice with over expression of TGFβ between postnatal day 7 and 14 (Vicencio et al., 2004). TGFβ signaling occurs via two serine/threonine kinase transmembrane receptors, TGFβR-I and –II, that act in sequence to phosphorylate and activate the transcription factors Smad2 and 3 (Bartram and Speer, 2004). GAG are known to enhance TGFβ cellular responses by preventing degradation of active TGFβ and stabilization of receptor binding, which is dependent on its sulfation state (Chen et al., 2007; Schultz and Wysocki, 2009). Our data demonstrates that there is an increase in TGFβ signaling in the *Sumf1*$^{-/-}$ mice. P-Smad levels were significantly increased at the onset of alveolarization (P5) and remained elevated at P10. In various models of arrest in alveolar formation it has been demonstrated that *in vivo in utero* injection of TGFβ neuralizing antibodies results in normal alveolar septation (Nakanishi et al., 2007; Neptune et al., 2003). In fact, *In utero* treatment of *Sumf1*$^{-/-}$ mice with TGFβ neutralizing antibodies lead to normal pSmad levels pos-natally, alveolar septation and lung function. Thus, our results indicate that sulfatases use different signaling pathway in cartilage (FGF) and lung (TGFβ) to fulfill their functions.

In summary, our data show that lack of sulfatase activity in the *Sumf1*$^{-/-}$ mice leads to a developmental arrest of alveolarization resulting in an emphysema-like phenotype. Furthermore, we demonstrated that proteoglycan desulfation is a negative regulator of TGFβ signaling during alveolar formation in mice. Our current hypothesis is that the increased sulfated state of GAG enhances and/or stabilizes TGFβ signaling. These findings support the hypothesis that ECM proteins serve critical roles in activation of different cytokine signaling pathways in distinct tissues. These data has potential clinical implication as it demonstrate lung parenchymal involvement in sulfatase deficiency.

4. Experimental Procedures

4.1. Animals

Sumf1$^{-/-}$, *FGF18*$^{-/-}$, and *FGFR3*$^{-/-}$ mice were previously described (Colvin et al., 1996; Liu et al., 2002; Settembre et al., 2007). Genotyping was performed by genomic PCR as described. For histomorphological studies, we examined ten *Sumf1*$^{-/-}$ mice at post-natal day 0 (P0), P5, P7, P10 and P30. Ten *Sumf1*$^{-/-}$;*FGF18*$^{+/-}$, and *Sumf1*$^{-/-}$;*FGFR3*$^{+/-}$ mice were examined at P10. Histological analysis of both lungs was consistent among all mice examined for a given genotype. All mouse protocols were approved by the Animal Care and Use Committee of Columbia University.

4.2. In Vivo Airway Measurements

Animal preparation. Sumf1$^{-/-}$ and WT 20 day old mice were anesthetized with an injection of pentobarbital sodium (60mg/kg i.p.). After tracheostomy, an 18-gauge metal cannula was inserted into the trachea and tightly bound with 4-0 nylon sutures. The mouse was connected via the tracheal cannula to a computer-controlled small animal ventilator (FlexiVent, Montreal, Canada) (Schuessler and Bates, 1995; Shalaby et al., 2010; Vanoirbeek et al.). Mice were mechanically ventilated at 150 breaths/min with a tidal volume of 8 ml/kg at a positive end-expiratory pressure (PEEP) of 3 cmH2O. Then the mice were paralyzed with an

injection of succinylcholine (10 mg/kg i.p.). Heart rate was monitored by a 3-lead electrocardiogram. A "snapshot perturbation" maneuver was applied to measure whole respiratory system (airways, lung, and chest wall) resistance (R), compliance (C), and elastance (E). Subsequently, a forced oscillation perturbation was applied, "primewave-8," and resulted in Raw, tissue damping (G), and tissue elastance (H). Ten mice per group were analyzed and all maneuvers and perturbations were performed in triplicate.

4.3. Tissue preparation

Mice were euthanized with isoflurane, lungs collected *en bloc* and inflated through the trachea with 4% paraformaldehyde at a pressure of 20 cm H_2O for 30 min. The trachea was ligated and the lungs fixed overnight in the same fixative. The lungs were washed in phosphate buffered saline (PBS), dehydrated and embedded in paraffin. To decreased shrinkage artifact the lung used for morphometric analyses were fixed as described above but with 2% paraformaldehyde;2% glutaraldehyde and embedded in methylmethacrylate.

4.4. Microscopic examination/Immunohistochemistry

Lung tissue slides were prepared and stained with hematoxylin and eosin, or Vehoeff's elastic fiber staining. GAG staining was performed on lungs fixed in methacarn and stained with acidic Alcian blue (pH 1), as previously described (Settembre et al., 2007). For immunohistochemistry, the paraffin was removed from 5 μm sections with xylene; sections were rehydrated through graded ethanol series, washed in water, boiled in 10mM sodium citrate buffer pH 6.0 and incubated with Sma2 (Cell Signaling #3122) primary antibody. Subsequently, the sections were washed in phosphate buffered saline and incubated with secondary antibody reagents according to the Vectastain Elite protocol for peroxidase labeling (Vector Laboratories). We applied NovaRed as a substrate using the Vector NovaRed Substrate Kit (Vector Laboratories) and counterstained with hematoxylin. The sections were dehydrated and mounted using DPX mount (Sigma). Negative controls were done in parallel by omitting the primary antibody. Positive immunoreactivity was determined by the intensity and distribution of staining.

4.5. Lung morphometry

For quantitative analysis of the distal airspace enlargement, we used stereological techniques as previously described (Ochs, 2006; Weibel et al., 2007). Lungs were fixed and embedded as described above. Five sequential 5μm transverse sections were collected every 200μm starting at the base of the lungs. Observations were made using a Leica DM 4000B microscope equipped with a Leica DFC300 FX digital camera. At least 5 areas per section and two sections per mouse were analyzed. Point counting was done using ImageJ 1.41o (NIH) with well over 200 points counted per mouse. Lung volumes were measured by the liquid displacement method (Hyde et al., 2007).

4.6. Western blotting and sulfated GAG assay

Lungs were collected from P0, P5, P7 and P10 mice, homogenized and lysed in Staph A lysis buffer (n=3 per each time point). Western blotting was done as previously described using pSmad (Cell Signaling #3101) and activin (Sigma) antibodies (Carta et al., 2009). Freshly collected P10 lungs were homogenized and sulfated GAG was quantified using the Blyscan kit (Biocolor, UK).

4.7. TGFβ neutralizing antibody treatment

Mice were treated as previously described (Neptune et al., 2003). In brief, 5mg/kg of TGFβ neutralizing antibody (R&D systems) was injected into pregnant *Sumf1*$^{+/-}$ female on

embryonic days 17 and 19. As control, we injected in the same fashion 5mg/kg rabbit IgG (Sigma). Four mice for each group were analyzed at P10.

4.8. Statistical Analyses

Statistical significance was assessed by Student's t test or a one-way ANOVA followed by Newman-Keuls test for comparison between more than two groups. A $p<0.05$ was considered significant (*$p<0.05$, **$p<0.01$, ***$p<0.001$).

Acknowledgments

This work was supported by grants from the NIH to Gerard Karsenty

We are indebted to Drs. D.M. Ornitz for providing FGF18 and FGFR3 deficient mice. E. A-S. thanks S. Lee-Arteaga for technical help and discussion through out the project. E. A-S is the recipient of a post-doctoral fellowship of the Cystic Fibrosis Foundation (USA). C. S. is the recipient of EMBO long-term postdoctoral fellowship. This work was supported by grants from the NIH to G.K.

References

Bartram U, Speer CP. The role of transforming growth factor beta in lung development and disease. Chest. 2004; 125:754–765. [PubMed: 14769761]

Bulow HE, Hobert O. The molecular diversity of glycosaminoglycans shapes animal development. Annu Rev Cell Dev Biol. 2006; 22:375–407. [PubMed: 16805665]

Carta L, Smaldone S, Zilberberg L, Loch D, Dietz HC, Rifkin DB, Ramirez F. p38 MAPK is an early determinant of promiscuous Smad2/3 signaling in the aortas of fibrillin-1 (Fbn1)-null mice. J Biol Chem. 2009; 284:5630–5636. [PubMed: 19109253]

Chailley-Heu B, Boucherat O, Barlier-Mur AM, Bourbon JR. FGF-18 is upregulated in the postnatal rat lung and enhances elastogenesis in myofibroblasts. Am J Physiol Lung Cell Mol Physiol. 2005; 288:L43–51. [PubMed: 15447937]

Chen Q, Sivakumar P, Barley C, Peters DM, Gomes RR, Farach-Carson MC, Dallas SL. Potential role for heparan sulfate proteoglycans in regulation of transforming growth factor-beta (TGF-beta) by modulating assembly of latent TGF-beta-binding protein-1. J Biol Chem. 2007; 282:26418–26430. [PubMed: 17580303]

Colvin JS, Bohne BA, Harding GW, McEwen DG, Ornitz DM. Skeletal overgrowth and deafness in mice lacking fibroblast growth factor receptor 3. Nat Genet. 1996; 12:390–397. [PubMed: 8630492]

Cosma MP, Pepe S, Annunziata I, Newbold RF, Grompe M, Parenti G, Ballabio A. The multiple sulfatase deficiency gene encodes an essential and limiting factor for the activity of sulfatases. Cell. 2003; 113:445–456. [PubMed: 12757706]

Dasgupta C, Sakurai R, Wang Y, Guo P, Ambalavanan N, Torday JS, Rehan VK. Hyperoxia-induced neonatal rat lung injury involves activation of TGF- {beta} and Wnt signaling and is protected by rosiglitazone. Am J Physiol Lung Cell Mol Physiol. 2009; 296:L1031–1041. [PubMed: 19304912]

Diez-Roux G, Ballabio A. Sulfatases and human disease. Annu Rev Genomics Hum Genet. 2005; 6:355–379. [PubMed: 16124866]

Esko JD, Lindahl U. Molecular diversity of heparan sulfate. J Clin Invest. 2001; 108:169–173. [PubMed: 11457867]

Faham S, Hileman RE, Fromm JR, Linhardt RJ, Rees DC. Heparin structure and interactions with basic fibroblast growth factor. Science. 1996; 271:1116–1120. [PubMed: 8599088]

Frese MA, Milz F, Dick M, Lamanna WC, Dierks T. Characterization of the human sulfatase sulf1 and its high-affinity heparin/heparan sulfate interaction domain. J Biol Chem. 2009

Galambos C, Demello DE. Regulation of alveologenesis: clinical implications of impaired growth. Pathology. 2008; 40:124–140. [PubMed: 18203035]

Grande JP. Role of transforming growth factor-beta in tissue injury and repair. Proc Soc Exp Biol Med. 1997; 214:27–40. [PubMed: 9012358]

Hyde DM, Tyler NK, Plopper CG. Morphometry of the respiratory tract: avoiding the sampling, size, orientation, and reference traps. Toxicol Pathol. 2007; 35:41–48. [PubMed: 17325971]

Kovensky J. Sulfated oligosaccharides: new targets for drug development? Curr Med Chem. 2009; 16:2338–2344. [PubMed: 19519394]

Lamanna WC, Frese MA, Balleininger M, Dierks T. Sulf loss influences N-, 2-O-, and 6-O-sulfation of multiple heparan sulfate proteoglycans and modulates fibroblast growth factor signaling. J Biol Chem. 2008; 283:27724–27735. [PubMed: 18687675]

Lin X. Functions of heparan sulfate proteoglycans in cell signaling during development. Development. 2004; 131:6009–6021. [PubMed: 15563523]

Liu Z, Xu J, Colvin JS, Ornitz DM. Coordination of chondrogenesis and osteogenesis by fibroblast growth factor 18. Genes Dev. 2002; 16:859–869. [PubMed: 11937493]

Massague J, Blain SW, Lo RS. TGFbeta signaling in growth control, cancer, and heritable disorders. Cell. 2000; 103:295–309. [PubMed: 11057902]

Nakanishi H, Sugiura T, Streisand JB, Lonning SM, Roberts JD Jr. TGFbeta- neutralizing antibodies improve pulmonary alveologenesis and vasculogenesis in the injured newborn lung. Am J Physiol Lung Cell Mol Physiol. 2007; 293:L151–161. [PubMed: 17400601]

Neptune ER, Frischmeyer PA, Arking DE, Myers L, Bunton TE, Gayraud B, Ramirez F, Sakai LY, Dietz HC. Dysregulation of TGF-beta activation contributes to pathogenesis in Marfan syndrome. Nat Genet. 2003; 33:407–411. [PubMed: 12598898]

Ochs M. A brief update on lung stereology. J Microsc. 2006; 222:188–200. [PubMed: 16872418]

Roth-Kleiner M, Post M. Similarities and dissimilarities of branching and septation during lung development. Pediatr Pulmonol. 2005; 40:113–134. [PubMed: 15965895]

Schuessler TF, Bates JH. A computer-controlled research ventilator for small animals: design and evaluation. IEEE Trans Biomed Eng. 1995; 42:860–866. [PubMed: 7558060]

Schultz GS, Wysocki A. Interactions between extracellular matrix and growth factors in wound healing. Wound Repair Regen. 2009; 17:153–162. [PubMed: 19320882]

Settembre C, Annunziata I, Spampanato C, Zarcone D, Cobellis G, Nusco E, Zito E, Tacchetti C, Cosma MP, Ballabio A. Systemic inflammation and neurodegeneration in a mouse model of multiple sulfatase deficiency. Proc Natl Acad Sci U S A. 2007; 104:4506–4511. [PubMed: 17360554]

Settembre C, Arteaga-Solis E, McKee MD, de Pablo R, Al Awqati Q, Ballabio A, Karsenty G. Proteoglycan desulfation determines the efficiency of chondrocyte autophagy and the extent of FGF signaling during endochondral ossification. Genes Dev. 2008; 22:2645–2650. [PubMed: 18832069]

Shalaby KH, Gold LG, Schuessler TF, Martin JG, Robichaud A. Combined forced oscillation and forced expiration measurements in mice for the assessment of airway hyperresponsiveness. Respir Res. 2010; 11:82. [PubMed: 20565957]

Sporn MB, Roberts AB. Transforming growth factor-beta: recent progress and new challenges. J Cell Biol. 1992; 119:1017–1021. [PubMed: 1332976]

Tomita H, Egashira K, Ohara Y, Takemoto M, Koyanagi M, Katoh M, Yamamoto H, Tamaki K, Shimokawa H, Takeshita A. Early induction of transforming growth factor-beta via angiotensin II type 1 receptors contributes to cardiac fibrosis induced by long-term blockade of nitric oxide synthesis in rats. Hypertension. 1998; 32:273–279. [PubMed: 9719054]

Usui H, Shibayama M, Ohbayashi N, Konishi M, Takada S, Itoh N. Fgf18 is required for embryonic lung alveolar development. Biochem Biophys Res Commun. 2004; 322:887–892. [PubMed: 15336546]

Vanoirbeek JA, Rinaldi M, De Vooght V, Haenen S, Bobic S, Gayan-Ramirez G, Hoet PH, Verbeken E, Decramer M, Nemery B, Janssens W. Noninvasive and invasive pulmonary function in mouse models of obstructive and restrictive respiratory diseases. Am J Respir Cell Mol Biol. 42:96–104. [PubMed: 19346316]

Vanoirbeek JA, Rinaldi M, De Vooght V, Haenen S, Bobic S, Gayan-Ramirez G, Hoet PH, Verbeken E, Decramer M, Nemery B, Janssens W. Noninvasive and invasive pulmonary function in mouse models of obstructive and restrictive respiratory diseases. Am J Respir Cell Mol Biol. 2010; 42:96–104. [PubMed: 19346316]

Vicencio AG, Lee CG, Cho SJ, Eickelberg O, Chuu Y, Haddad GG, Elias JA. Conditional overexpression of bioactive transforming growth factorbeta1 in neonatal mouse lung: a new model for bronchopulmonary dysplasia? Am J Respir Cell Mol Biol. 2004; 31:650–656. [PubMed: 15333328]

Weibel ER, Hsia CC, Ochs M. How much is there really? Why stereology is essential in lung morphometry. J Appl Physiol. 2007; 102:459–467. [PubMed: 16973815]

Weinstein M, Xu X, Ohyama K, Deng CX. FGFR-3 and FGFR-4 function cooperatively to direct alveogenesis in the murine lung. Development. 1998; 125:3615–3623. [PubMed: 9716527]

Yamamoto T, Takagawa S, Katayama I, Nishioka K. Anti-sclerotic effect of transforming growth factor-beta antibody in a mouse model of bleomycininduced scleroderma. Clin Immunol. 1999; 92:6–13. [PubMed: 10413648]

Highlights

In this study we demonstrate using a mouse model of multi sulfatase deficiency, *Sumf1*$^{-/-}$, that sulfatases play an important role in alveolar formation and lung function. We identified that high levels of sulfated glycosaminoglycans lead to upregulation of the TGFβ and anti-TGFβ therapy leads to normal lung development and function in *Sumf1*$^{-/-}$ mice.

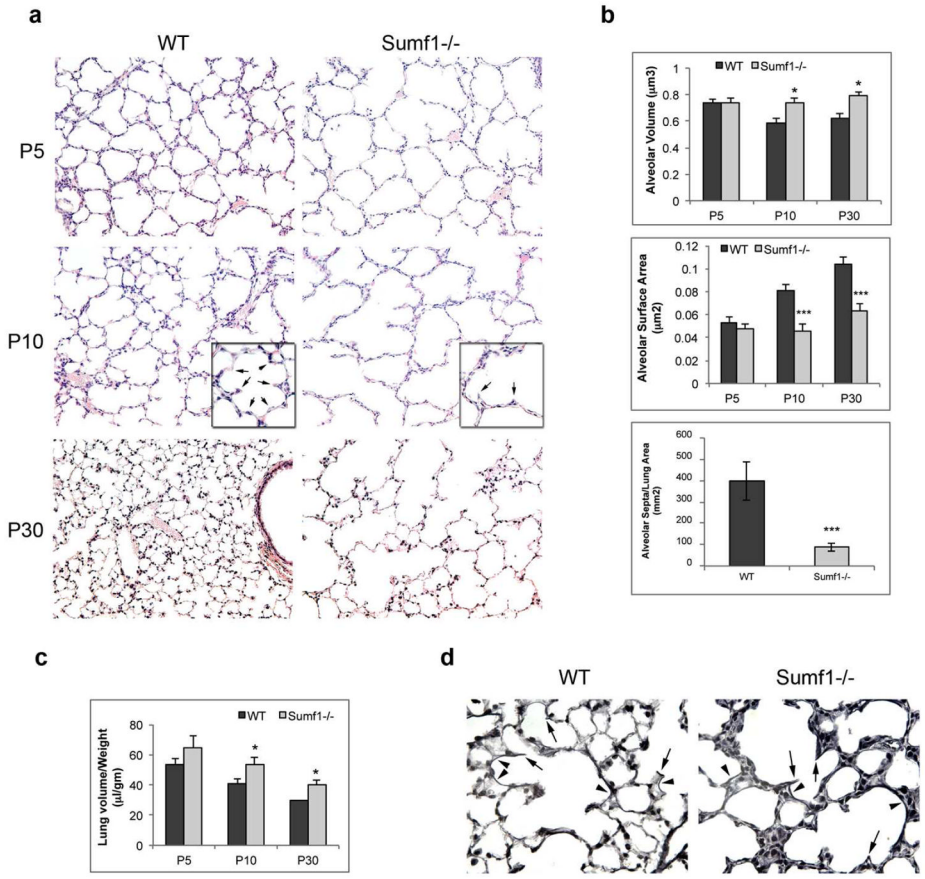

Figure 1.

Lung histopathology and morphometry of wild type (WT) and *Sumf1*$^{-/-}$ mice. **a-**Lung sections from WT and *Sumf1*$^{-/-}$ littermates at P5, P10 and P30 illustrates an increase in distal airspace caliber at P10 and P30 in the *Sumf1*$^{-/-}$ compared to the WT (Magnification is 200x). High power magnification (400x) of lung sections at P10 (insert) indicate decreased alveolar septal tips (arrows) in the *Sumf1*$^{-/-}$ compared to the WT. **b-**Lung morphometric analysis done using stereological techniques demonstrates that the *Sumf1*$^{-/-}$ lungs has a statistically significant increase in alveolar volume and a concomitant decrease in alveolar surface area and alveolar septal tip number (septal tip densities were calculated at P10). **c-**Lung volume normalized to total body weight is statistically significantly increased in P5 and P10 *Sumf1*$^{-/-}$ compared to WT mice. n=10 for each group, *p<0.05, ***p<0.001, error bars represent standard deviations. **d-**Verhoeff elastic staining demonstrates normal elastic fibers in the alveolar walls (arrow heads) and tip of the secondary septa (arrows) in P10 *Sumf1*$^{-/-}$ compared to WT mice (200x magnification).

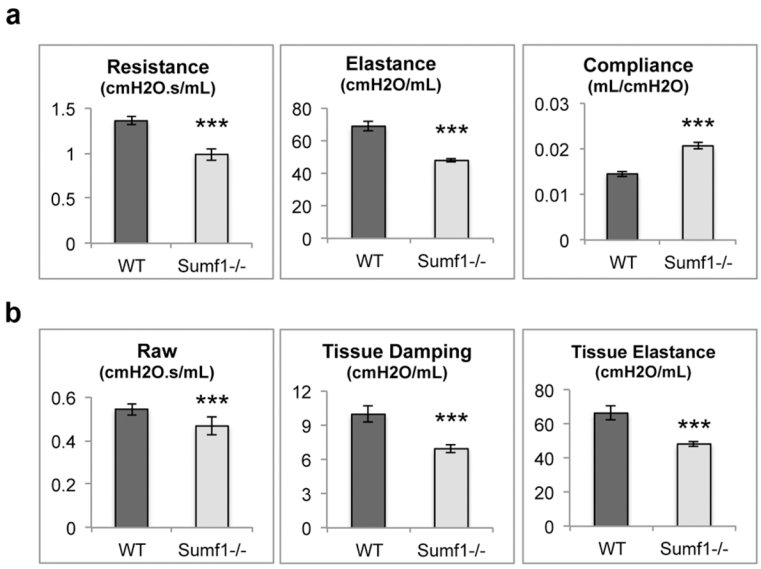

Figure 2.

In vivo lung function analysis demonstrates that the *Sumf1*$^{-/-}$ lungs have similar physiological properties as an emphysema lung. The *Sumf1*$^{-/-}$ mice demonstrate a 27% decrease in resistance ($p<0.0001$), 30% decrease in elastance ($p<0.001$), and a 42% increase in compliance ($p<0.001$). Additionally, the *Sumf1*$^{-/-}$ mice were noted to have a 14% decrease in airway resistance (Raw) ($p<0.01$), a 30% decrease in tissue damping, and a 27% decrease in tissue elastance. n=10 for each group, ***P<0.001, error bars represent standard deviations.

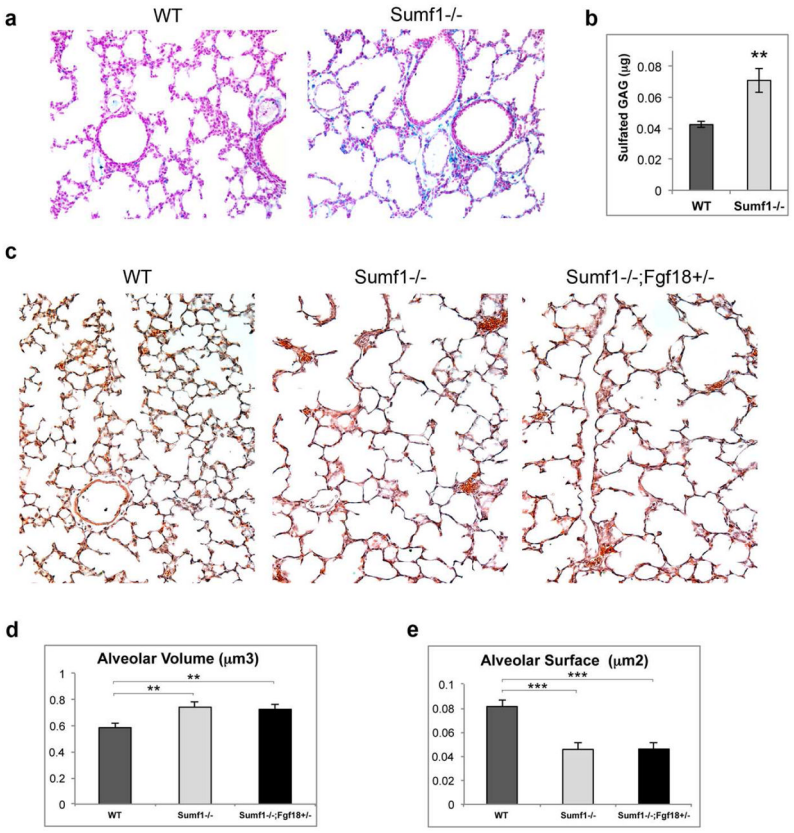

Figure 3.

Deposition of sulfated GAG in *Sumf1*$^{-/-}$ lungs affects alveolar formation in an FGF-independent manner. **a-**Metacarn fixed and acidic alcian blue stained lungs demonstrate an increase in deposition of sulfated GAG in the *Sumf1*$^{-/-}$ lungs (blue staining) compared to the wild type (WT) littermate at P10 (Magnification 200x). **b-**Biochemical analysis demonstrates a 67% increase in sulfated GAG in the *Sumf1*$^{-/-}$ lung compared to WT. **c-** H&E sections demonstrates that removal of on allele of *FGF18* in the *Sumf1*$^{-/-}$ (*Sumf1*$^{-/-}$;FGF18$^{+/-}$) mice failed to rescue alveolar septation at P10 (Magnification is 200x). **b-**Lung morphometric analysis demonstrate that the *Sumf1*$^{-/-}$ and *Sumf1*$^{-/-}$;FGF18$^{+/-}$ lungs were undistinguishable. n=10 for each group, **p<0.01, ***p<0.001, error bars represent standard deviations.

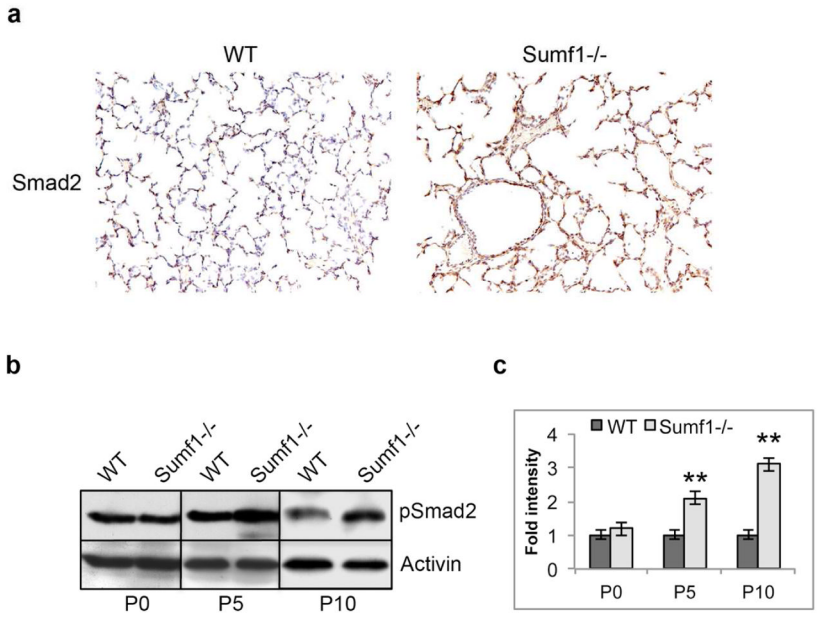

Figure 4.

TGFβ signaling in lung tissue of mice deficient in Sumf1. **a**-Immunohistiochemical analyses of lung sections from wild type (WT) and *Sumf1*$^{-/-}$ littermates at P10 illustrate an increase in Smad2 (brown staining) in the *Sumf1*$^{-/-}$ lungs compared to WT littermates. **b**-Western analysis at the stated stages demonstrated increased p-Smad activity in *Sumf1*$^{-/-}$ compared to the WT whole lung protein extract at P5 and P10. **c**-Western analysis band quantification demonstrates a 2 fold and 3 fold increase in p-Smad signaling in *Sumf1*$^{-/-}$ compared to WT at P5 and P10. n=5 for each group, **p<0.01, error bars represent standard deviations.

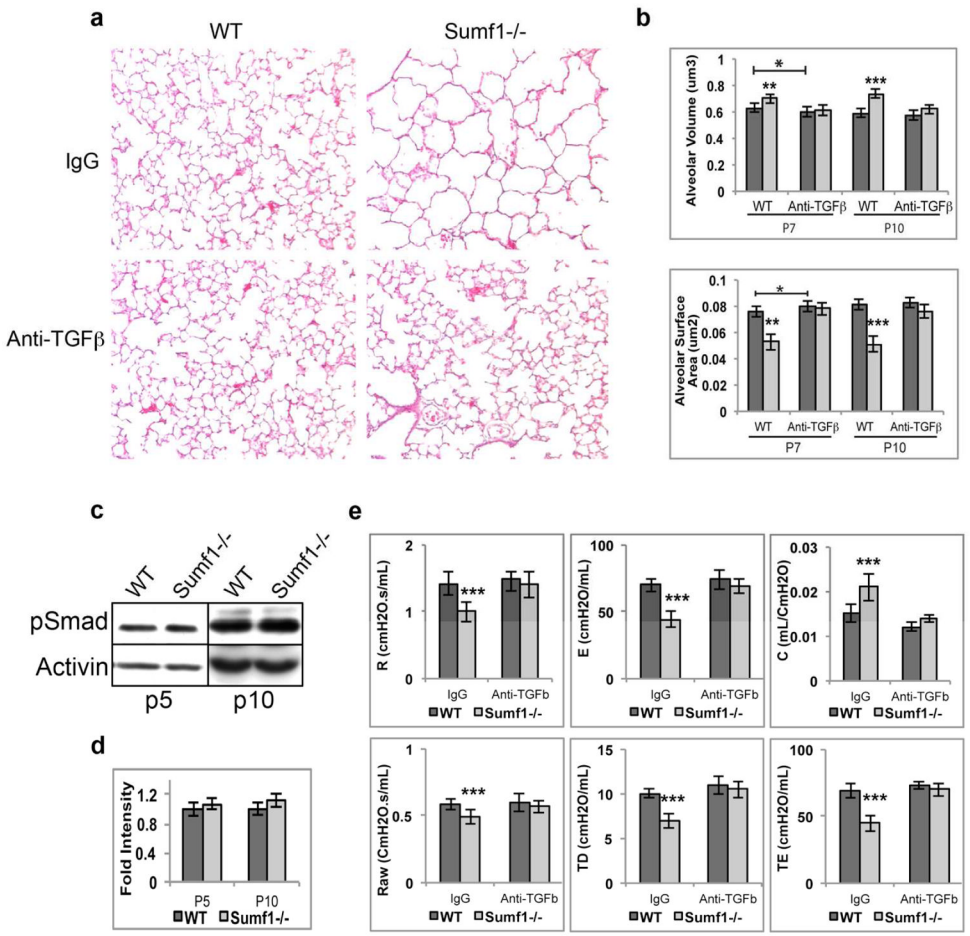

Figure 5.

Neutralization antibody to TGFβ rescues alveolarization in *Sumf1*$^{-/-}$ mice. **a**-H&E stained lung sections from wild type (WT) and *Sumf1*$^{-/-}$ littermates at P10 treated *in utero* with TGFβ neutralizing antibodies demonstrate a rescue of alveolar septation compared to rabbit IgG treated mice (Magnification is 200x). **b**-Lung morphometric analyses demonstrate normalization of the alveolar surface area and alveolar volume in the *Sumf1*$^{-/-}$ lungs treated with neutralizing antibodies. In addition, we detected a statistically significant decrease in alveolar volume and an increase in alveolar surface area in TGFβ treated WT compared to IgG treated mice at P7 but not at P10. **c**-TGFβ treatment normalized p-Smad levels in *Sumf1*$^{-/-}$ lung at P5 and P10. **d**-Western analysis band quantification demonstrates comparable levels of p-Smad in TGFβ neutralizing antibody treated *Sumf1*$^{-/-}$ compared to WT mouse lung at P5 and P10. **e**-*In vivo* lung function analyses demonstrate that treatment with TGFβ neutralizing antibodies normalizes resistance (R), elastance (E), compliance (C), airway resistance (Raw), tissue damping (TD) and tissue elastance (TE) in *Sumf1*$^{-/-}$ mice, whereas, IgG treatment had no effect. N=5 per group, ***=P<0.001, error bars represent standard deviations.